

Aerodynamic Flow Separation Control Using Plasma Actuator of Rectangular Cross Section with a Side Ratio of $B/D=2$

著者	Matsuda Kazutoshi, Kato Kusuo, Suda Kentaro, Imamura Mitsushi, Cao Nade
journal or publication title	Proceedings of 13th UK Conference on Wind Engineering
page range	1-4
year	2018-09-03
URL	http://hdl.handle.net/10228/00006938

Aerodynamic Flow Separation Control Using Plasma Actuator of Rectangular Cross Section with a Side Ratio of $B/D=2$

Kazutoshi Matsuda^{1*}, Kusuo Kato¹, Kentaro Suda¹, Mitsushi Imamura¹, and Nade Cao¹

¹Department of Civil Engineering and Architecture, Kyushu Institute of Technology, Kitakyushu, Fukuoka, Japan

**matsuda@civil.kyutech.ac.jp*

INTRODUCTION

In order to suppress wind-induced vibrations of bridge girders, two general methods are applied: aerodynamic and mechanical countermeasures. In this study, a new approach to suppress wind-induced vibrations, "a dielectric barrier discharge (DBD) plasma actuator", was investigated through wind tunnel experiments to determine its potential as a device for flow control around bridge deck sections. This approach is already in use in other fields, such as in the fluid dynamics flow control for separation control in wing surface flow. The DBD plasma actuator [1] is an electric device designed for flow control that utilizes the DBD effect. Figure 1 shows a schematic illustration of the DBD plasma actuator and its mechanism of flow control. As shown in our previous research results [2, 3], air flow control effect using the plasma actuator is qualitatively confirmed by the experiments of flow visualization of motion-induced vortex-induced vibration and Kármán vortex-induced vibration in their onset reduced wind speed regions on the forced-oscillating rectangular cross-section. However, it has not been quantitatively confirmed yet if the air flow control actually affects aerodynamic vibration. Therefore, this research was conducted aiming at quantitatively confirming the vibration control effect on aerodynamic vibration using a plasma actuator by a spring-supported test on the rectangular cross-section of the side ratio of $B/D = 2$. Furthermore, the flow visualization experiment was conducted under the condition where a model of a rectangular cross-section of a spring-supported test system was aerodynamically vibrated and the differences in the patterns of flows around the cross section caused by the existence and non-existence of the control by plasma actuator were confirmed. It was found that the vibration control method using a plasma actuator was proven to quantitatively have more vibration control effect than without using any countermeasure from the result of a spring-supported test targeted at the rectangular cross-section of the side ratio of $B/D = 2$.

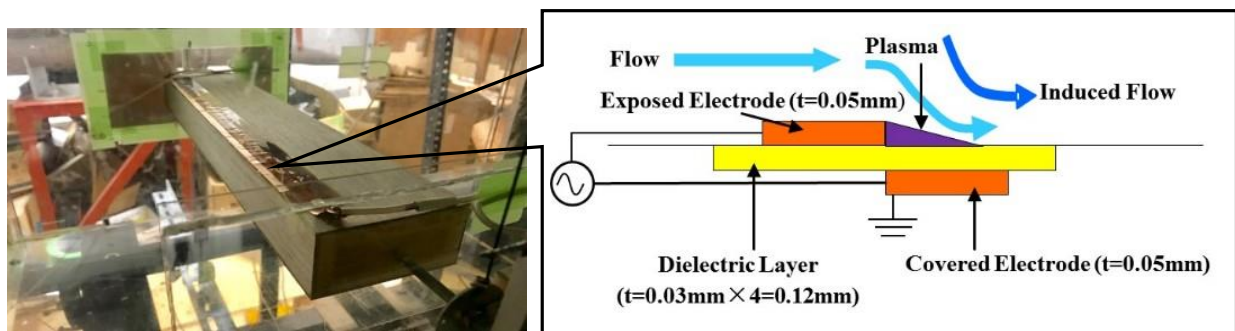


Figure 1: Dielectric Barrier Discharge Plasma actuator

EXPERIMENTAL SETUP

Table 1 shows the specifications of the DBD plasma actuator used in the research. The same experimental condition of the plasma actuator is applied for all the experiments. Spring-supported test and smoke flow visualization were carried out for on and off controlled states of the plasma using a 0.4m x 0.4m wind tunnel at Kyushu Institute of Technology. Table 2 shows an experimental conditions for spring-supported tests. All wind tunnel tests were performed in a smooth flow.

Table 1: Specifications of Plasma Actuator

AC Frequency		4kHz
AC Voltage		±4kV
Electrode	Material	Copper
	Thickness	0.05mm
	Width	5mm(exposed) 10mm(covered)
Overlap of Electrode		0mm
Dielectric Layer	Material	Polyimide
	Thickness	0.03mm × 4 =0.12mm
	Width	25mm
Duty Cycle		100%

Table 2: Experimental Conditions for Spring-supported Tests

B (mm)	D (mm)	Side Ratio B/D	Sc =2mδ/ρD²	f (Hz)	Plasma Actuator (PA)
80	40	2.0	4.2	3.26	ON
					OFF
				7.22	ON
					OFF

RESULTS AND DISCUSSION

The results of the comparison of the responses in motion-induced vortex vibration due to the existence or non-existence of the control by plasma actuator (PA) are shown in Figures 2. The vertical axis is set as non-dimensional double amplitude $2\eta/D$ (η : amplitude (m) and D : model height (m)), and the horizontal axis is set as reduced wind speed $Vr = V/fD$ (V : wind speed (m/s), f : natural frequency (Hz) and D : model height (m)). The numbers in the figure show the control rate of response $\{ = (\text{response at the time of PA-OFF} - \text{response at the time of PA-ON}) / (\text{response at the time of PA-OFF}) \times 100 \}$. In the case of $f = 7.22\text{Hz}$ of Figure 2, the vibration control effect by PA in the wind speed region of motion-induced vortex vibration could be confirmed. It was revealed that the vibration control rate was higher on the side with high wind speed and the effect of the vibration control by PA is larger on the side with high wind speed. It is considered to be due to the amplitude dependency of aerodynamic force in the wind speed region of motion-induced vortex vibration. Figure 3 shows a time history response where the control rate of response is 39% at $Vr=5.5$ in Figure 2. Furthermore, from the results of the experiment of flow visualization as shown in Figure 4, because the control of separated vortex from the leading edge was observed at the time of PA-ON, the airflow control effect by PA could be confirmed. The arrow points to the position where PA is installed. Figure 5 shows that the vibration control effect by PA was confirmed in the Kármán vortex-induced vibration wind speed region. Figure 6 indicates flow visualization test results of free oscillating model where the control rate of response is 83% at $Vr=13.8$ in Figure 5. The control of Kármán vortex was observed as the same trend of the case of separated vortex from the leading edge as shown in Figure 4.

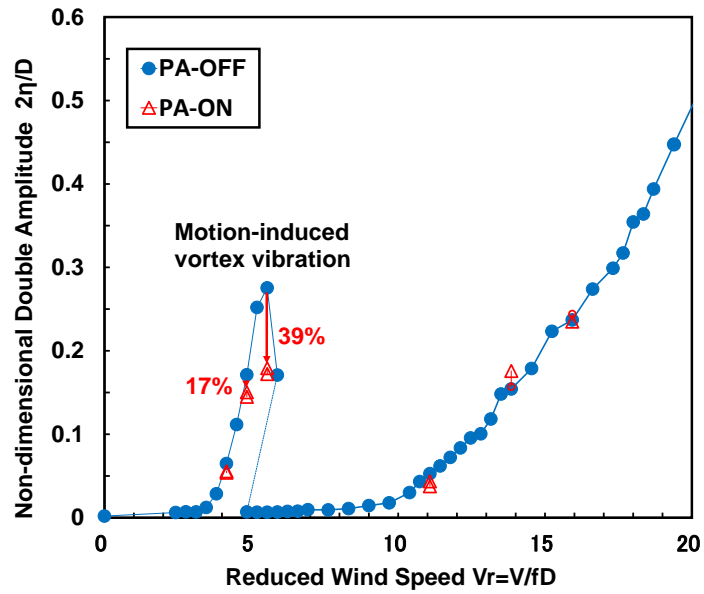


Figure 2: Spring-supported Test Result ($f=7.22\text{Hz}$)

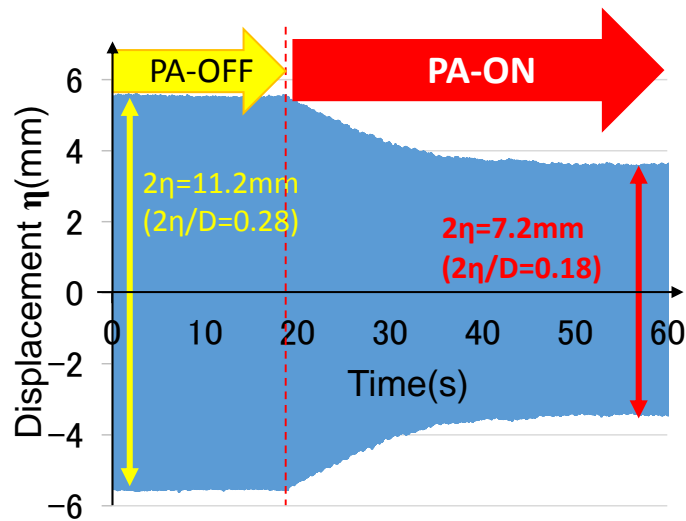
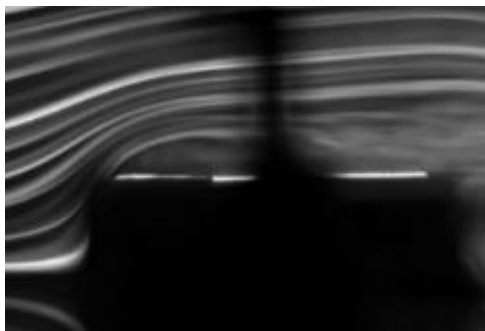
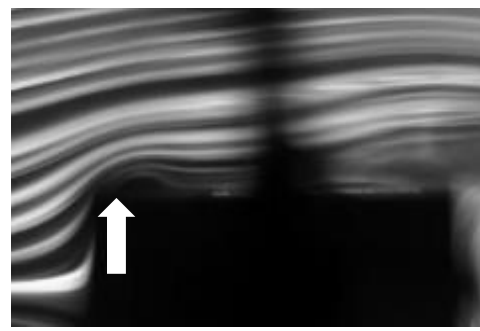


Figure 3: Time History Response at $Vr=5.5$ ($f=7.22\text{Hz}$)



(a) PA-OFF, $2\eta/D = 0.28$



(b) PA-ON, $2\eta/D = 0.17$

Figure 4: Flow Visualization Test Results of Free Oscillating Model of $B/D=2.0$ at the Top Displacement at $Vr=5.5$, $f=7.22\text{Hz}$ (motion-induced vortex vibration wind speed region)

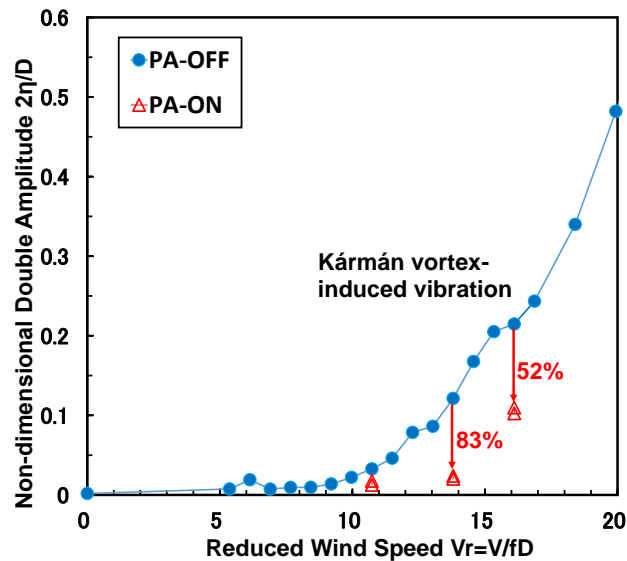


Figure 5: Spring-supported Test Result ($f=3.26\text{Hz}$)

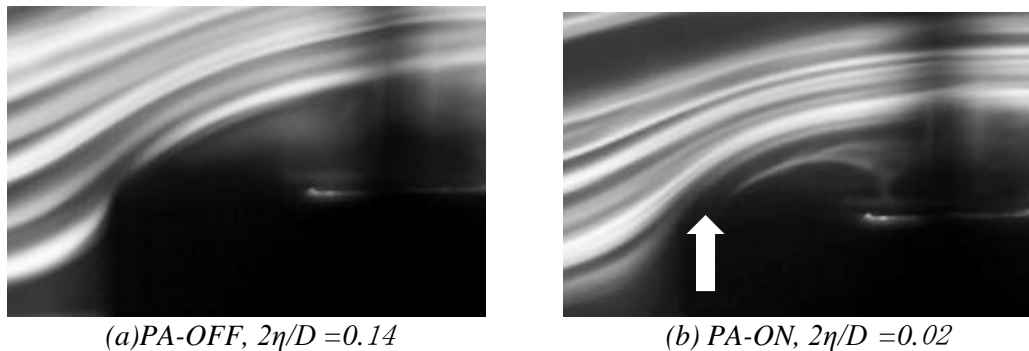


Figure 6: Flow Visualization Test Results of Free Oscillating Model of $B/D=2.0$ at the Top Displacement at $V_r=13.8$, $f=3.26\text{Hz}$ (Kármán vortex-induced vibration wind speed region)

CONCLUSIONS

This research was conducted aiming at quantitatively confirming the vibration control effect on aerodynamic vibration using a plasma actuator by a spring-supported test on the rectangular cross-section of side ratio of $B/D = 2$. As a result, the vibration control effect could be confirmed to some extent on both motion-induced vortex vibration and Kármán vortex-induced vibration.

ACKNOWLEDGEMENTS

This work was supported by JSPS KAKENHI Grant Number 16K06470.

REFERENCES

- [1] Corke T.C., Enloe C.L. & Wilkinson S.P. (2010). "Dielectric Barrier Discharge Plasma Actuators for Flow Control", *Annual Review of Fluid Mechanics*, **42**, 505–529.
- [2] Matsuda K., Kato K., Uchida T., Hirano C. & Sawata A. (2013). "Flow Control of Bridge Deck Sections Using Dielectric Barrier Discharge Plasma Actuator", *Proceedings of the 6th European-African Conference on Wind Engineering*.
- [3] Matsuda K. & Kato K. (2015). "Aerodynamic Flow Separation Control of Bridge Deck Sections Using Plasma Actuators", *Proceedings of the ASME 2015 Pressure Vessels & Piping Division Conference*, PVP2015-45140.